ICARUS 77, 311–329 (1989)

The Neutral Cloud and Heavy Ion Inner Torus at Saturn

R. E. JOHNSON,* M. K. POSPIESZALSKA,* E. C. SITTLER, JR.†
A. F. CHENG,‡ L. J. LANZEROTTI,§ AND E. M. SIEVEKA*

*Department of Nuclear Engineering and Engineering Physics, University of Virginia, Charlottesville, Virginia 22901; †Goddard Space Flight Center, Greenbelt, Maryland 20771; ‡Johns Hopkins University Applied Physics Laboratory, Laurel, Maryland; and §AT&T Bell Laboratories, Murray Hill, New Jersey 07974

Received December 23, 1987; revised June 6, 1988

Saturn has a torus of neutral water molecules and dissociated water molecule products (OH and O) which coexists with the icy satellites and the E-ring. Here we calculate the morphology of this cloud using Voyager plasma data and recent laboratory data on water molecule sputter yields and energy distributions. In this model the icy satellites are sources of sputtered water vapor. The molecules so produced co-orbit with the satellites, forming a cloud of neutrals. This cloud can act to limit the amount of H^+ close to the orbital plane, via charge exchange, and it is the source of the heavy ion plasma via ionization. The plasma production rates are also calculated and show a structure with distance from Saturn and with distance from the orbit plane which suggests that the heavy ion plasma is not equilibrated inside $\sim 7R_S$. The source rates are consistent with ion lifetimes of $\sim 10^6$–10^7 sec near Dione and Tethys; however, they clearly indicate that additional sources of plasma are required inside $\sim 4R_S$. Finally, we examine the possibility that the E-ring may be a precipitate of this neutral cloud initiated by low-energy ion–molecule reactions.

INTRODUCTION

The exciting discoveries of the heavy ion plasma tori of Jupiter and Saturn demonstrate that a unique coupling exists between the surface mineralogy of the satellites of these planets and the magnetospheric plasmas (Johnson *et al.* 1985; Cheng *et al.* 1986). The surfaces of objects imbedded in a magnetosphere are sources of neutrals (via micrometeorite bombardment, volcanos, and plasma ion sputtering). These neutrals are ionized and then swept up by the rotating planetary magnetic fields. The newly created ions then become a component of the plasma which flows onto the satellite surface (or, in the case of Io, the atmosphere), producing sputtering and/or collisional ejection of additional material. Therefore, the planetary magnetospheric plasma can become self-sustaining. More importantly for planetary science, a description of the plasma can lead to understanding of the surface mineralogy (Clark *et al.* 1986) or, vice versa, knowledge of surface materials can lead to a description of plasma production and characteristics (Cheng *et al.* 1986).

Both Pioneer (Frank *et al.* 1980) and Voyager (Bridge *et al.* 1981, 1982; Lazarus and McNutt 1983; Richardson 1986; Krimigis *et al.* 1981, 1983) spacecraft detected a torus of heavy ions in the vicinity of the icy satellites of Saturn. Limits on mass discrimination of the particle analyzers made it difficult to distinguish in much of this region whether the ions were nitrogen, oxygen, or for that matter a water or ammonia ion product, such as OH^+, NH_3^+, etc. The possible presence of both nitrogen and oxygen on the moons is suggested by models of their formation and by surface features. At Saturn's distance from the Sun the primary volatile species expected is water ice. How-

0019-1035/89 $3.00

ever, ammonia is expected to be mixed in a clathrate or other form and the tidal heating of this mixture may account for much of the geology of the objects (Stevenson 1982; Moore 1984). Clark *et al.* (1984) have observed the reflectance spectra and identified water ice as a primary constituent of the inner Saturnian satellites but no positive identification of an ammonia component has been made. This may be due to the fact that the plasma ion bombardment of the surface itself obscures the ammonia-in-ice feature, as suggested by Lanzerotti *et al.* (1984).

Nitrogen has also been suggested as a possible constituent for this torus, supplied by inward diffusion from the Titan torus. However, Richardson (1986) has suggested that the heavy ions between 14 and $17R_S$ are water group ions moving outward from the satellites. The only positive identification of an atomic component of this torus was the EUV result of Wu *et al.* (1980). They claimed to have observed excited O^{2+} and give a net source rate of 8×10^{25} oxygen ions/sec, but this observation was not confirmed by Voyager.

The presence of the icy satellites led Cheng and Lanzerotti (1978), and subsequently others, to suggest that the bombardment of the satellites by the ions may be the source of fresh neutrals via sputtering and of new ions from ionization of these neutrals. This self-supply would be balanced by loss processes (diffusion, charge exchange, electron–ion recombination, etc.), creating the plasma densities observed. This line of thought has been used by Richardson *et al.* (1986) and Huang and Siscoe (1987) to create models for the net ion content of the torus. Micrometeorite bombardment is also a source of neutral ejecta. This is a small effect for the outer icy satellites (Cheng *et al.* 1986; Haff and Eviatar 1986; Haff *et al.* 1983) but may be important for objects or rings within $\sim 4R_S$ (Northrop and Connerney 1987).

In all of the calculations presented here we will treat the sputtering as resulting from a low-temperature water (<100°K) ice surface. We earlier published sputter yields and escape fractions determined from laboratory measurements of the sputtering of low-temperature water ice (Lanzerotti *et al.* 1983, erratum). These experiments have clearly demonstrated that neutral whole molecules are the dominant ejecta when sputtering water ice (Brown *et al.* 1984; Reimann *et al.* 1984; Bar-Nun *et al.* 1985; Chrisey *et al.* 1986). For energetic ions incident on a low-temperature ice (<100°K) these neutrals are predominantly H_2O with a small admixture of O_2,H_2 (Brown *et al.* 1984) and some radicals (Haring *et al.* 1984; Bar-Nun *et al.* 1985). Although the majority of the sputtered H_2O molecules are ejected with sufficient energy to escape the weak gravitational fields of the small icy satellites they are not, for the most part, energetic enough to escape Saturn's gravitational field. Therefore, the ejected neutral molecules will co-orbit with the satellites until ionized by UV photons, plasma electrons or by charge exchange with other ions. The orbiting neutrals form an extended atmosphere for these satellites in much the same way the ejected Na forms a cloud co-orbiting with Io about Jupiter. However, the lower plasma and UV fluxes in the Saturnian system are such that the neutrals make a number of complete orbits, on the average, prior to ionization. Therefore, as described by Barton (1983), Johnson *et al.* (1984, 1985), Cheng *et al.* (1986), and Richardson *et al.* (1986), these neutrals form a roughly azimuthally symmetric torus of water molecules and dissociation products in the vicinity of the satellites. Such an atmosphere, derived from the satellites and occupying the same region of space, is gravitationally bound to Saturn.

In the process of calculating the morphology of this neutral cloud we also determine the supply rate of heavy ions to the inner torus. This is of considerable importance in understanding the observed plasma temperatures and density profiles in the inner

plasma torus as pointed out by Johnson *et al.* (1984). Therefore, describing the neutral cloud appropriately is important for determining, for instance, the possible need for additional sources of heavy plasma and the local lifetimes of the plasma ions.

The region of space subtended by this neutral cloud (extended atmosphere) is also occupied by the diffuse E-ring (Baum *et al.* 1981). It has been pointed out (Cheng *et al.* 1986; Johnson *et al.* 1984; Haff *et al.* 1983) that the plasma ions can rapidly (~within 10^3–10^4 years) erode the small, micron-sized particles which are thought to make up this interesting feature. Recently, we evaluated these rates using the Pioneer and Voyager plasma data and laboratory sputtering yields giving accurate estimates of this erosion (Johnson *et al.* 1984; Lanzerotti *et al.* 1983, erratum). However, the E-ring particles can also accrete materials from the neutral torus (Johnson *et al.* 1984). Therefore, in this paper, we examine the competition between accretion and sputter erosion of the E-ring particles. The inclusion of possible accretion is important in finally determining whether this ring is a long-lived feature of the present icy component of the Saturnian system or is a geologically ephemeral feature possibly produced by an event at Enceladus.

SPUTTER FLUXES

Experimental yields for the ejection of water molecules from thin films of ice due to incident protons and to incident ions with masses near that of oxygen are summarized in Fig. 1a for ice temperatures <80°K. These data span the range from slow ion bombardment, <1 keV/amu, for which collisional sputter ejection dominates, to much faster ions for which electronic excitation and ionization energy loss leads to sputter ejection. In all cases the yields are given for perpendicular incidence to the surface normal. For nonnormal incidence these yields are enhanced by $(\cos \alpha)^{-n}$, where $1 \leq n < 2$ and α is the angle the ions make with the surface normal. This enhancement persists out to some angle at which surface roughness limits ejection. To account for the rough regolith on the satellites (Hapke 1986) we use the results in Fig. 1a directly, ignoring any enhancement, a procedure suggested by Sieveka and Johnson (1982) for icy surfaces (Johnson 1988).

The relative amounts of $H_2(D_2)$ and O_2

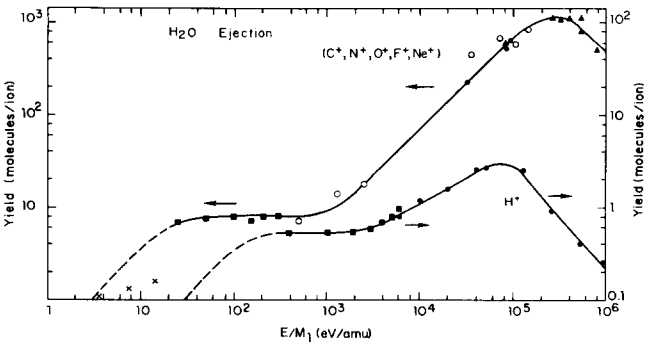

FIG. 1a. An accumulation of the sputtering yields for low-temperature (<80°K) water ice from a variety of published data: (●) Brown *et al.* (1984); (○) N^+, Bøttiger *et al.* (1980); (▲) F^+, Cooper and Tombrello (1984) scaled by $(\cos 30°)^{1.6}$ to correct for nonnormal incidence; (■) H^+, Ne^+, Bar-Nun *et al.* (1985) scaled to Brown *et al.* (1984) data for protons; (×) Ne^+, Chrisey *et al.* (1986). E is the incident ion energy and M is ion mass in amu. Left-hand axis is for O^+-like ions, right-hand axis for H^+. Solid line connecting data points obtained using models for extrapolating sputtering data (Johnson *et al.* 1984; Lanzerotti *et al.* 1983). The dashed line is an extrapolation using $Y \approx 0.01\ (E/U)$, $U = 0.52$ eV. (×) Simulation calculation (Brenner and Garrison 1986), gives lower limit to yield in this region.

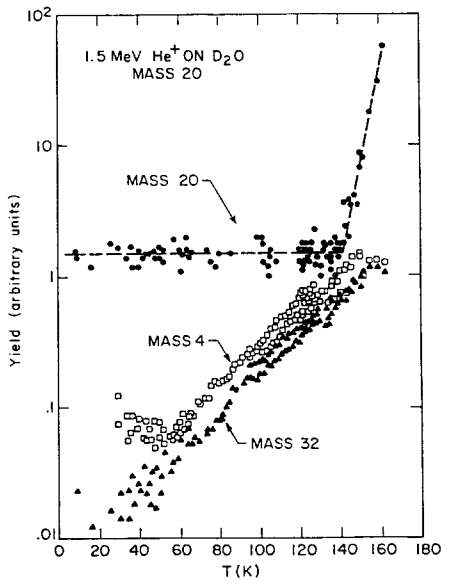

FIG. 1b. Relative yields of D_2O (mass 20), D_2 (mass 4), and O_2 (mass 32) ejected from D_2O ice by 1.5-MeV He^+ (a) (Brown *et al.* 1984) vs substrate temperature at fluence of $\sim 10^{15}$ ions/cm^2.

ejected vs substrate temperature for mega- and kilo-electron volt incident ions is shown in Fig. 1b. These yields depend on irradiation time (Reimann *et al.* 1984) and the absolute yields of the individual species are difficult to ascertain. However, the relative yields are representative and it is seen from the temperatures in Table I that a small but nonnegligible amount of H_2 and O_2 may be ejected from the sunlit hemispheres, based upon the expected maximum surface temperatures. We do not treat the H^+ plasma created by the hydrogen products, but neglect of the O_2 in the following means our numbers are *lower limits* on the heavy neutral torus.

In Table I the orbital kinetic energies are given at those distances from Saturn at which the important icy satellites orbit. (This energy is also equal to the additional energy required for escape from Saturn's system.) Also given is the kinetic energy of rotation of the ions attached to the rotating field of Saturn. Based on these energies and Figs. 1a and b it is seen that even in the absence of a significant plasma temperature the ions will bombard and sputter the surfaces of these satellites none of which have thick atmospheres. It is also noteworthy that the corotation speed exceeds twice the orbital speed at $2.33R_S$, which is close to the outer limit of the main ring system. Therefore, an ion which is neutralized at larger distances from Saturn may be lost from the system. This process may be important for limiting ring formation beyond $2.33R_S$. The magnetic field corotation en-

TABLE I

SATELLITE PARAMETERS

	Radial position, R_S[a]	Radius (km)	T_{max} (°K)[b]	U_s H_2O (eV)	Orbital frequency, τ_0^{-1} (sec^{-1})	Corotation energy (eV/amu)	Orbital energy (eV/amu)	Critical energy, $O^+(H^+)$[c] (keV)	Escape fraction of H_2O, f_e
Mimas	3.08	197	~101	0.003	1.2×10^{-5}	4.8	1.0	55(880)	0.99
Enceladus	3.95	251	75 ± 3	0.004	8.3×10^{-6}	8.0	0.80	21(340)	0.98
Tethys	4.88	524	93 ± 4	0.015	6.1×10^{-6}	12.1	0.65	26(420)	0.95
Dione	6.26	559	~101	0.024	4.2×10^{-6}	20.	0.51	6.8(110)	0.91
Rhea	8.74	765	100 ± 2	0.041	2.5×10^{-6}	40.	0.37	1.7(27)	0.83

[a] R_S is Saturn's radius (6.03×10^4 km); the magnetospheric rotation frequency is 2.6×10^{-5}/sec.

[b] T_{max} determined from visual albedo A, $T_{max} = [(1 - A)F_0/\sigma\varepsilon]^{1/4}$, F_0 is solar flux, σ is the Stephan–Boltzman constant, and $\varepsilon \approx 1$.

[c] Energy of ion with gyroradius equal to satellite radius; much faster ions bombard isotropically, much slower ions flow onto the trailing hemisphere.

ergy is of interest as a freshly produced ion, which is accelerated to gyrate around the magnetic field lines, will also attain an amount of gyration energy equivalent to its velocity relative to the field. This energy "heats" the plasma.

Voyager measurements by the Low Energy Charged Particle (LECP) experiment indicated the presence of a hot plasma (>30 keV) (Krimigis *et al.* 1983), which will also sputter the surface. The nature of the net flow onto the surface for the cold and hot components of the plasma is determined by the gyroradii of the ions, the pitch angle distribution, and their incident speed (Pospieszalska and Johnson 1987). If the gyroradius is much less than the satellite's radius, and if the mean thermal speed of the ions is much less than the relative speed between the magnetic field and the satellite, then the plasma will bombard the trailing hemisphere of the satellite. Otherwise, bombardment may occur over the entire surface of the satellite, particularly if the ions have motion along the field lines. In either limit, the net sputter source rate from the satellite averaged over the surface is

$$J_s \approx f_e n_i \langle v_i Y(v_i) \rangle (\pi R^2). \quad (1)$$

Here f_e is the escape fraction, n_i is the ion number density, and $\langle v_i Y(v_i) \rangle$ is the impact velocity times the sputtering yield, averaged over the incident velocity spectrum.

The critical energy at which the ion gyroradius is equal to the satellite radius is also given in Table I. The hot ion energy spectrum measured by the LECP instrument has its largest density at the low-energy limit of detection (~30 keV at Saturn). It is seen from Table I that the hot protons in this spectrum will bombard the trailing side, whereas the hot O^+ in this spectrum will bombard nearly isotopically at Dione and Rhea (Pospieszalska and Johnson 1988). In all cases the cold plasma (<100 eV) preferentially bombards the trailing hemisphere. The overall preferential bombardment of the trailing hemisphere is also suggested by the reflectance spectra of Clark *et al.* (1984).

In describing the local satellite surface source distribution of sputter species, the distribution of bombarding ions and the nature of the paths by which the escaping H_2O molecules leave the gravitational field of the satellite are not treated in detail. Sieveka and Johnson (1984) described the gravitational influence of the satellite on the effective exit velocity distribution of SO_2 at Io. The influence of gravity tends to average the source distribution over the surface. Because of this, and because of the importance of the oxygen component in the hot plasma, we initially assume isotropic ejection of the escaping molecules, calculating the net flux from Eq. 1. We also calculate the neutral torus assuming only trailing hemisphere ejection, to examine the sensitivity to the source distribution of the calculated neutral cloud morphology.

The energy spectra of ejected molecules also have been measured (Reimann *et al.* 1984; Haring *et al.* 1983; Chrisey *et al.* 1986). Such results can be used to calculate the fraction of the sputtered H_2O escaping from these objects, f_e, as listed in Table I. The energy spectra of water molecules sputtered from the surface with energy between E and $E + dE$ has the form $2EU/(E + U)^3$ (Reimann *et al.* 1984), where U is an empirically determined parameter, ~0.05 eV for incident O^+-like ions (Chrisey *et al.* 1986). Escape from the satellite's gravitational influence requires that $E \geq U_s$, the satellite escape energy, in Table I. As $U \gg U_s$ for most of the satellites, the escape fractions, $(2X + 1)/(X + 1)^2$, $X = U_S/U$, are close to unity. The energy distribution for molecules entering the torus becomes $2(E + U_s)U/(E + U_s + U)^3$.

In Table II are given the net sources from each satellite using the escape fraction in Eq. 1 and the yields in Fig. 1a. These sources are calculated for the fluxes obtained from the Pioneer and Voyager measurements as described in the footnote to the table (Lanzerotti *et al.* 1983, erratum).

TABLE II

SATELLITE SPUTTER FLUXES OF H_2O^a BY INCIDENT O^+ AND NET SATELLITE RATES

	Pioneer	Voyager cold	Voyager 1 hot	Voyager 2 hot	Source rate used, J_S (mole/sec)
		(10^8 $H_2O/cm^2/sec$ = $\mu m/10^3$ year)			
Mimas	0	0			0
Enceladus	0.03	0.8[b]		1.0[b]	1.4×10^{24}
Tethys	0.7	1.0[b]	4[b]	0.6	1.7×10^{25}
Dione	2.0[b]	1.3	6[b]	0.6	3.2×10^{25}
Rhea	0.07	0.5[b]	2[b]	0.2	2.0×10^{25}
Total					7.0×10^{25}

[a] Flux obtained using Eq. (1) (divided by satellite area) and Fig. 1. Pioneer estimates [see Fig. 2 of Johnson *et al.* (1984)]. Voyager 1 and 2 hot plasma (Lanzerotti *et al.* 1983, erratum); these plasma data were not extrapolated to the plane of satellite orbits, but for each satellite erosion rate, measurements closest to this plane were used. Hot plasma was assumed predominantly O^+. Cold plasma obtained based on new Richardson and Sittler (1988) averages and extrapolations of the Voyager data sites.

[b] Fluxes used as estimates of total flux times satellite area to give J_S for our calculation, i.e., largest estimates of the cold and hot components, as discussed in text.

The differences between Voyagers 1 and 2 in Table II are due mainly to differences in spacecraft latitude. The "cold" data in Table II are estimated using the extrapolation of Voyager PLS ion densities to the orbital plane using the model of Richardson and Sittler (1988). These are reasonably consistent with each other and with the Pioneer data, except at Rhea where Pioneer was farthest from the plane. This would imply that although electron temperatures, etc., may be variable, the ion-induced sputter source rate is fairly consistent using these data sets. Therefore, for the source rates here we use a sum of the hot (LECP) data at the point closest to the plane in each case and the largest "cold" contribution. The total yields are still *lower limits* due to the lack of availability of hot plasma data at all energies and the fact they are not extrapolated to the orbit plane. The H_2O source rates used for each satellite are given in Table II. The total source used is seen to be $\sim 7.0 \times 10^{25}$ H_2O/sec. This also means that after dissociation, $\sim 10^{26}$ H^+ are supplied to the proton torus.

MODEL

H_2O molecules are assumed to be ejected isotropically in the satellite's rest frame at a rate and with an energy spectrum described in the previous section. The molecules injected into the torus have the satellite orbital velocity as well as the sputter velocity. This forms the initial condition for new molecules entering the torus. Because the satellites are small compared to the orbital scale (and the spheres of influence are not much larger), we ignore the effect of the satellites on the ejected molecules. The validity of this is tested later.

If the initial orbital energy and position are such that the molecules can escape Saturn or can intercept the main ring system, these molecules will quickly be lost from the neutral cloud and are not included in the determination of the cloud density. We ignore molecules with apoapsis $>25R_S$ or periapsis $<2.5R_S$. The fractions of the source distribution so eliminated are given in Table III. Using the source rates in Table II gives a total mass of 6×10^{15} kg (isotropic) or 2×10^{15} kg (trailing) added to the main ring system in 4.5×10^9 years compared to the much larger total ring mass of $\sim 3 \times 10^{19}$ kg. All other molecules are presumed to orbit Saturn, in a manner determined by their initial conditions, until they are ionized. Once ionized their subsequent motion is determined by the magnetic field the ions are added to and heat the plasma as described above.

The neutral molecules are ionized by

TABLE III

	Fraction of sputtered H_2O escaping Saturn[a,b]	Fraction of sputtered H_2O intercepting rings[b]	Fraction of sputter fluxes swept up by satellites[b]
Enceladus	2×10^{-4} (0)	2.4×10^{-2} (8×10^{-2})	0.03 (0.04)
Tethys	3×10^{-3} (0)	1×10^{-2} (3×10^{-2})	0.06 (0.08)
Dione	8×10^{-3} (0)	9×10^{-3} (2×10^{-2})	0.02 (0.03)
Rhea	4×10^{-2} (0)	6×10^{-3} (2×10^{-2})	0.01 (0.02)

[a] Includes particles with orbits extending beyond $25R_S$. Calculations based on 5000 particles per satellite.

[b] Parentheses imply trailing hemisphere bombardment.

photons, plasma electrons, and plasma ions (via charge exchange). The rates for ionization have been estimated by several authors (Barton 1983; Eviatar *et al.* 1983; Johnson *et al.* 1984; Richardson *et al.* 1986). It is found that the molecular lifetimes against ionization are much longer than the orbital periods. Therefore, sputtered molecules will generally contribute to the neutral cloud for a number of orbits. This allows a convenient simplification. Because the satellites are assumed to continuously emit sputtered molecules throughout their orbits, and because these molecules live for many orbits, they provide, on the average, a toroidal source. Therefore, the cloud is assumed to be azimuthally symmetric around Saturn. This is opposite to the case for Na at Io (Smyth 1979), where an Na cloud of limited extent co-orbits with Io because of the high rate of ionization of Na in that plasma environment. However, even at Io, the longer-lived neutral O torus, though peaked at Io's position, is significantly distributed azimuthally (Smyth and Shemansky 1983).

As photons and plasma electrons can also dissociate molecules, the orbital motion of the molecules may be modified prior to the species being lost from the neutral cloud. In this calculation we will describe the fate of the heavy species (O, OH from H_2O or N, NH, NH_2 from NH_3). Therefore, we treat, for example, H_2O, OH, and O as equivalent. In a dissociative process, such as $H_2O + h\nu \rightarrow H + OH + \Delta E$ (Table IV), the H atom carries off most of the center-of-mass kinetic energy change. The OH fraction of the energy is $(1/18)\Delta E$, with ΔE typically ~1–2 eV. These energies are much smaller than the orbital energies, although comparable to the sputtered molecule energies. The velocity change experienced by the heavy fragment is also small. As these dissociations occur randomly throughout the cloud of orbiting molecules, the principal effect is to smooth the calculated density distribution somewhat.

The ejected molecules can have orbits that are inclined to the satellite orbit plane, and may reside well outside this plane for a considerable time. This clearly does not modify the photoionization rate. However, as the plasma densities have scale heights which can be a fraction of an R_S, this can be very important for the electron ionization and charge exchange rates. Because sputtering is the source of this plasma, the problem should be solved in a self-consistent manner. To consider this we use the spatial distribution of the plasma computed by Richardson and Sittler (1988) to determine the ionization rates of sputtered neutrals and, thereby, the plasma source rates. These source rates are then compared to the measured and extrapolated ion densities in Fig. 8.

TABLE IV

PHOTOIONIZATION AND DISSOCIATION RATES AT SATURN[a]

$H_2O + h\nu \rightarrow O + H$	8×10^{-8} sec^{-1}
$OH + h\nu \rightarrow O + H$	8×10^{-8} sec^{-1}
$H_2O + h\nu \rightarrow H_2 + O$	2×10^{-8} sec^{-1}
$H_2O + h\nu \rightarrow H_2O^+ + e$	3×10^{-9} sec^{-1}
$OH + h\nu \rightarrow OH^+ + e$	9×10^{-9} sec^{-1}
$O + h\nu \rightarrow O^+ + e$	2×10^{-9} sec^{-1}

[a] Richardson *et al.* (1986).

In the model by Richardson and Sittler (1988) the plasma is assumed to be composed of a cold and hot electron component and cold H^+ and O^+ ions. The model is a representation of a composite of the Voyager 1 and 2 PLS ion and electron data using the analysis of these results by Richardson (1986) and Sittler *et al.* (1983). In order that azimuthal symmetry be obeyed in the Voyager 1 data, they assume constant flux tube content, N, and assume that inside $\approx 8R_S$, the ions exhibit the large pressure anisotrophy $T_\perp/T_\parallel \approx 5$ derived from the Voyager 2 ring plane crossing (Lazarus and McNutt 1983) and from Voyager 1 inbound and outbound observations (Richardson and Eviatar 1988). The model self-consistently solves for the amipolar electric field and includes the centrifugal and magnetic

mirror force terms. The ion and electron densities along the spacecraft trajectories are self-consistently calculated by requiring charge neutrality and assuming their observed differences are due to spacecraft charging. The model also assumes a dipole magnetic field and that the ion and electron temperatures are constant along the field lines.

As described in Sittler *et al.* (1983) a dramatic cooling of the plasma electrons was observed by the Voyager 2 PLS instrument inside $L = 5R_S$; this cooling was attributed to inelastic collisions with Saturn's E-ring but could also be due to the presence of neutral molecules (Eviatar 1984). As a result the cold electron component moved below the 10-eV low-energy cutoff of the PLS instrument and estimates of n_e and T_e for this component are not available within this inner region. However, during the ring plane crossing at $L \approx 2.8R_S$, the PLS instrument did detect a very thin plasma sheet of O^+ ions with scale height $H \approx 0.26R_S$ and maximum density ≈ 100 cm^{-3} (Lazarus and McNutt 1983). To compute these densities Richardson and Sittler (1988) assumed that the flux tube content was preserved (i.e., $N = n_e L^3 H$ = constant with H being the plasma sheet scale height), which allowed them to extrapolate their estimates for the cold ion and electron densities between $L = 4.8R_S$ and $L = 2.8R_S$.

We emphasize that the Voyager 2 trajectory was far off the ring plane for most of the encounter trajectory with z/H_0^+ ratios ~ 2, where z is the perpendicular distance above the ring plane. The only exception to this was near closest approach at $2.8R_S$ where the spacecraft crossed the ring plane at near normal incidence. This makes the extrapolation to the ring plane more difficult; for example, a large latitudinal gradient in $T_\perp/T_\parallel$ with maximum at the magnetic equator could cause one to underestimate equatorial densities (Richardson and Sittler 1988). We do note, due to recent analysis of PLS electron data in the Io torus by Sittler and Strobel (1987), that other dynamical phenomena producing $E_\parallel$ may also be present.

Using the spatial distributions of n_e and T_e for the cold and hot components from Richardson and Sittler (1988) we determine the ionization rate of the neutrals. This loss of neutrals limits their lifetime in the cloud but also gives the source rate of fresh ions and of plasma heating as described earlier. Therefore, at the end we compare in Fig. 8 these source rates to the plasma model used. We emphasize that because individual sputtered molecules sample a broad region of space the estimated spatial distributions and temperatures of the electrons used should give reasonable average ionization rates. The effect of uncertainties is discussed in the next section.

The electron ionization rates used for H_2O are given in Fig. 2. They are calculated from the total ionization cross-section data of Orient and Srivastava (1984) up to 400 eV and from the data of Schutten *et al.* (1966) in the range 400–10^4 eV. [Recently, Miller *et al.* (1987) have given accurate values of H_2O ionization which are consistent with those of Schutten *et al.* (1966).] That is, the rate constants shown in Fig. 2 are obtained, as is usual, by numerically integrating

$$k = \int_0^\infty v\sigma(v) f(v)\, dv \qquad (2)$$

where $f(v)$ is a Maxwell–Boltzman distribution for the appropriate electron temperature and σ is the ionization cross section. The results of Miller *et al.* (1987) show the branching ratio for $H_2O + e \rightarrow HO + H^+ + 2e$ to be 10% of the total ionization cross section. Here we ignore this. In addition we use the ionization rates for H_2O to approximate the rates for the dissociated water species also. The calculated values in Fig. 2 are consistent with those presented by Richardson *et al.* (1986) in the range 1–50 eV.

The charge exchange contribution to the neutral ionization rate is also estimated from the plasma model. For the cold

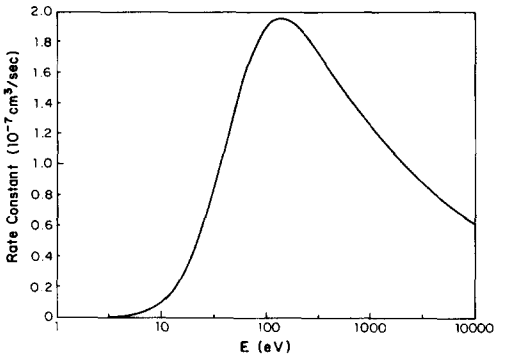

FIG. 2. Electron impact ionization rate constants versus temperature in electron volts. Calculated as described in the text.

plasma, charge exchange depends critically on the ionization energy differences between the incident ions and the neutrals (Johnson and Strobel 1982). We initially assume that the plasma ions are fully dissociated, i.e., H^+ and O^+. Within our knowledge of the neutral densities these can be assumed to have the same electron attachment energies. Therefore, the cold plasma charge exchange with fully dissociated neutrals (e.g., O) is a quasi-resonant process with high cross section. On the other hand, very low energy (<15 eV/amu) charge transfer of these species with H_2O (ionization energy ~12.5 eV) becomes small unless the H^+ or O^+ orbit the H_2O due to the attractive polarization forces. For the faster H^+ and O^+ measured by the LECP instrument the importance of the ionization energy difference diminishes and relatively large cross sections are obtained until such velocities that the momentum change of the transferred electron becomes important. Because we do not keep track of the dissociated water products, we use in the calculation an average charge transfer cross section $\sim 10^{-15}$ cm^2 for all of the plasma ions (Johnson and Strobel 1982).

The above approximation for charge exchange is very rough inside about $4R_S$. In this region the relative velocity between the cold ions and an orbiting neutral decreases. Ion–molecule orbiting collisions become likely (Johnson 1982; Johnson and Strobel 1982) so that the ion and neutral share the center of mass speed before separating. This reduces the average neutral exit speed and changes its direction. The neutrals, so formed, exit relatively slowly and, therefore, could contribute to the neutral cloud densities. As these neutrals have low relative speeds with respect to the plasma ions they also have high probabilities for subsequent charge exchange. For these reasons we also perform the calculation of the neutral densities ignoring charge exchange.

A summary of the ionization rates used is given in Fig. 3 as a function of Saturn radii in the plane of the orbiting satellites. These rates are seen in all cases to be much smaller than the inverse of the orbital periods in Table I, justifying the assumption of an azimuthally symmetric neutral torus.

ORBIT CALCULATIONS

A Monte-Carlo procedure is used to select orbits from the energy and angular distribution of molecules ejected from each moon. The initial coniditions for the test particle so chosen determine the two-body orbit about Saturn. If the orbit energy, when combined with the satellite motion, is large enough to lie well outside the volume of interest ($R > 25R_S$) or to intersect the main ring system ($R < 2.5R_S$) the particle is

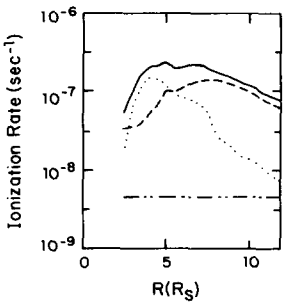

FIG. 3. Ionization rates calculated for the volume elements in Fig. 5 which are located in the satellite orbital plane. (–·–) Solar, (– – –) electron impact, (···) charge exchange; (—) total.

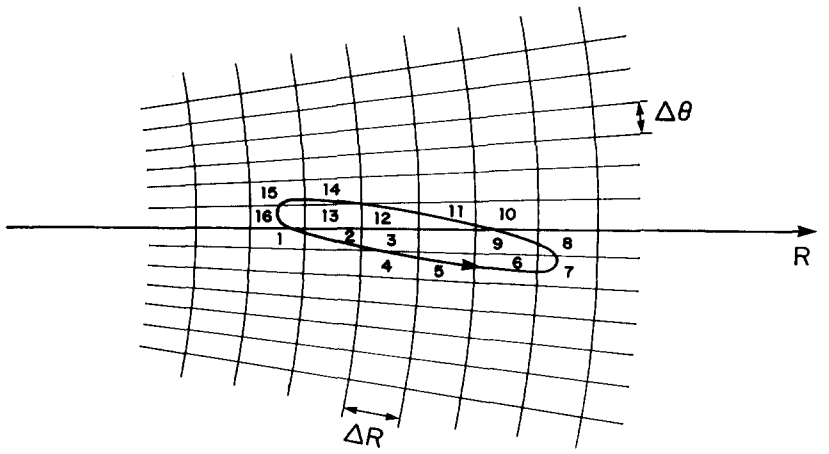

FIG. 4. The region around Saturn divided into boxes ($\Delta R = 0.25R_S$, $\Delta\theta = 1.5°$) and the projection of an orbit for a test particle from Enceladus onto the plane. The numbers denote the order in which a particle passes through the boxes in making one complete orbit about the planet.

not included in subsequent calculations.

The space about Saturn is divided into radial, R, and angular, θ, regimes, as shown in Fig. 4. This assumes an azimuthally symmetric source and neutral cloud as discussed earlier. For any of the boxes of Fig. 4 (rotated in ϕ about Saturn's axis) the net ionization rate (τ_i^{-1}) is calculated using

$$\tau_i^{-1} = (\tau_i)_{h\nu}^{-1} + (\tau_i)_{el}^{-1} + (\tau_i)_{ct}^{-1} \qquad (3)$$

where the right-hand side is a sum of the various processes contributing (photoionization, electron impact ionization, and charge transfer; Fig. 3). A test particle is tracked in its orbit. If this orbit goes through m boxes (see Fig. 4) then the orbit time is equal to $\Sigma_{i=1}^{m}\Delta t_i$ where Δt_i is the time spent in the ith box. For Markov chains, the probability of the particle having reached box $k + 1$ ($k \leq m$) in the first orbit without being ionized is

$$p^1(k) = \Pi_{i=1}^{k} \exp(-\Delta t_i/\tau_i) \qquad (4)$$

where τ_i^{-1} is the ionization rate in box i. The particle is tracked through its orbit, yielding a probability of surviving a single orbit of p_0. After n orbits the survival probability in box k is the value in Eq. (4) times $(p_0)^n$. Therefore, the total time spent in box k becomes $t(k) = \Delta t_k p^1(k)/(1 - p_0)$. Now the average contribution to the neutral number density in box k is obtained by

$$\Delta n_k = J_s t(k). \qquad (5)$$

Here, J_s is the net source (sputter) rate associated with the test particle energy, angle, and satellite. The source rates for each satellite are those given in Table II.

The net number density in each volume is obtained from the above by summing over contributions from all selected test particles and is displayed in Figs. 5a and b for isotropic and trailing hemisphere ejection, respectively. Five thousand particles were typically chosen for emission from each satellite, as larger numbers were found to not significantly change the cloud morphology. In addition to calculating the number densities we also display the ionization source rates in Figs. 6a and b for isotropic and trailing hemisphere ejection, respectively. These are equal to the neutral number densities times the local ionization rate τ_i^{-1} in Eq. (3). As $1 - p_0$ is small (i.e., the particle lives for many orbits), $t(k)$ is roughly proportional to n_e^{-1}, since the electron and ion impacts dominate the lifetime

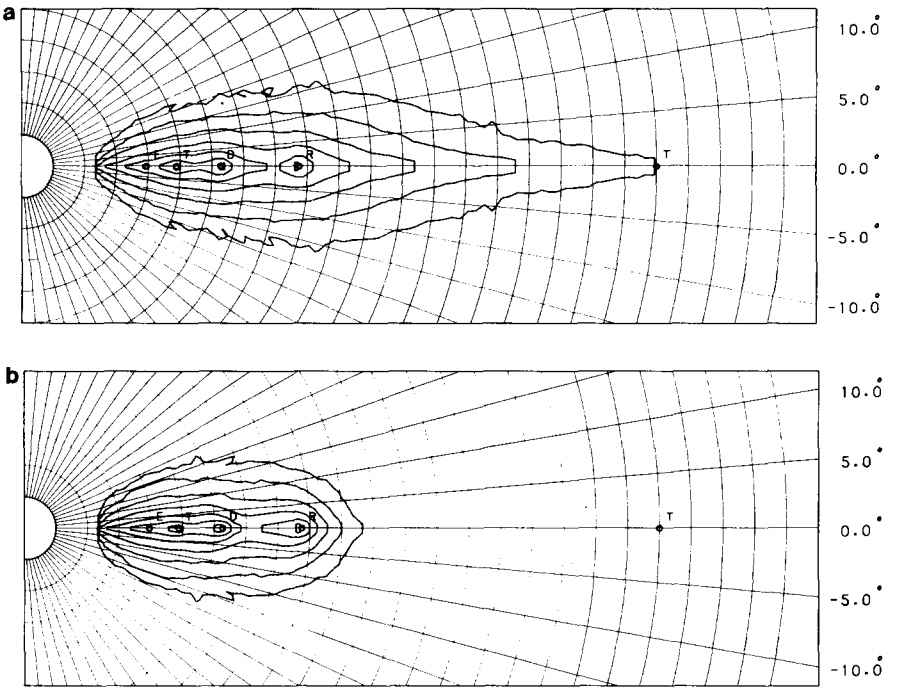

FIG. 5. Density of neutral torus of H_2O (O, OH, etc.) given as contours of equal density. Outer contour is a density of $10^{-1.5}$ moles/cm^3, and contours correspond to increasing powers by 0.5. (a) Isotropic ejection of H_2O from satellites. Densities in boxes containing satellites are 11 moles/cm^3 (Enceladus), 44 moles/cm^3 (Tethys), 36 moles/cm^3 (Dione), and 11 moles/cm^3 (Rhea). (b) Trailing hemisphere ejection ($\cos\beta$ from antapex of motion on the trailing hemisphere) with same net flux as in (a). Densities near satellites: 23 moles/cm^3 (Enceladus), 60 moles/cm^3 (Tethys), 44 moles/cm^3 (Dione), and 12 moles/cm^3 (Rhea).

in Eq. (3) (viz., Fig. 3). As J_s is also roughly proportional to n_i, the neutral number density contributions calculated in Eq. (5) would *not* be very sensitive to the uncertainties in the plasma density if the sputter source was determined by the dominant plasma component. The calculated neutral densities are affected both by changes in T_e, via $(\tau_i)_{el}$, and by the ion energies, which affect the sputter yields in Table II. The net source rate of new plasma ions is roughly equal to the total sputter yield, whereas the local rate directly depends on the local plasma density via $(\tau_i)_{el}$.

We also calculated the net flux of neutral material onto a small orbiting "test" surface passing through the cloud. This is calculated in two limits. The orbit is assumed to be that of, first, a neutral object in a gravitationally bound orbit and, second, a small charged particle corotating with the magnetosphere. This is done to bracket the likely behavior of the very small charged particles which might accrete material to form the E-ring grains. In Fig. 7 the net change in thickness of a grain due to this flux is compared to the calculated erosion rate of the grains based on the sputter fluxes in Table II.

RESULTS

It is seen from Figs. 5a and b that the neutral number densities are highly peaked about the orbital location of the satellite sources. The high local densities imply that there will be some sweeping of the neutrals

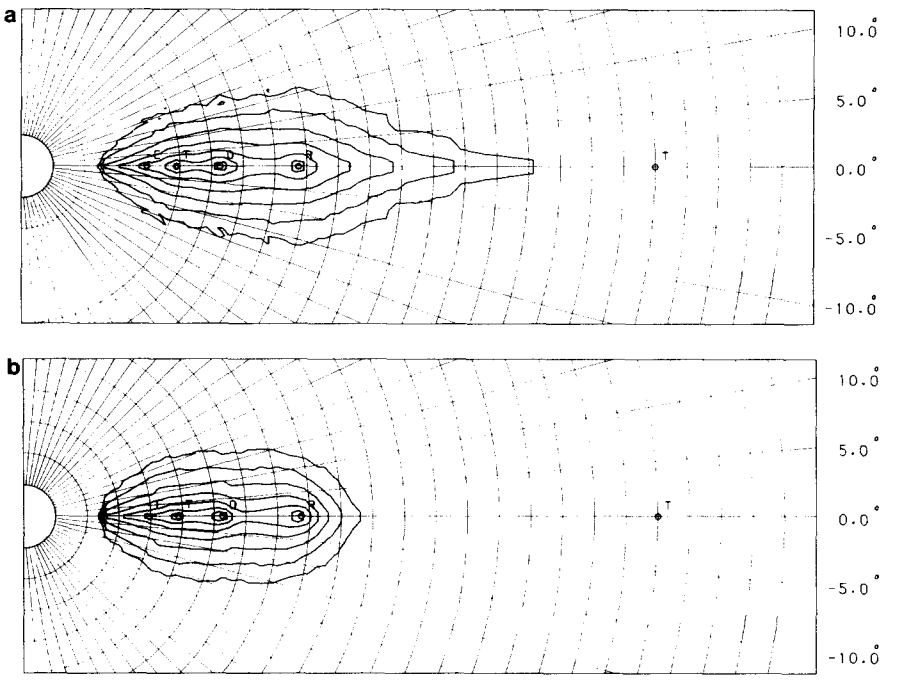

FIG. 6. Source rate of heavy ions in inner torus given as contours of equal source rate. Outer contours = $10^{-8.5}$ ions/(cm^3 sec) and contours correspond to increases in the power by 0.5. (a) Isotroipc ejection (as in Fig. 6a): source rates near satellites are 5.7×10^{-7} ions/cm^3/sec (Enceladus), 4.0×10^{-6} ions/cm^3/sec (Tethys), 4.5×10^{-6} ions/cm^3/sec (Dione), and 1.5×10^{-6} ions/cm^3/sec (Rhea). (b) Trailing hemisphere ejection (as in FIg. 6b): source rates near satellites are 1.1×10^{-6} ions/cm^3/sec (Enceladus), 5.5×10^{-6} ions/cm^3/sec (Tethys), 5.3×10^{-6} ions/cm^3/sec (Dione), and 1.6×10^{-6} ions/cm^3/sec (Rhea).

by the satellites. A rough limit on the size of this effect is obtained using the neutral flux in Fig. 7. This depletion is given in Table III using a radius of influence equal to half of the Lagrange sphere for each satellite (Sieveka and Johnson 1982). It is seen that less than 10% of the ejected flux is likely to be returned to the satellite, well within the uncertainties of our source rate. In competition with this, the dissociation of molecular species will tend to smooth the cloud density variations, as discussed earlier.

It is seen from Figs. 5a and b that although the neutral satellite atmosphere is large, it does not extend to the vicinity of Titan with any significant density. The principal component of the neutral cloud lies close to the orbital plane, as shown by Johnson *et al.* (1984). The neutral cloud in Fig. 5a is very similar in density and structure to the calculation presented in Cheng *et al.* (1986) in which the ionization rates were treated approximately, but the densities are much larger than those presented earlier in which proton sputtering was assumed to dominate (Barton 1983; Eviatar *et al.* 1983; Johnson *et al.* 1985). Removing charge exchange as a loss mechanism does not drastically change the morphology but does considerably increase the neutral densities in the inner region (~40/cm^3 near Enceladus, ~100/cm^3 near Tethys, ~60/cm^3 near Dione).

The effect of assuming trailing hemisphere ejection is to reduce the average orbital energies of the ejected H_2O so that the cloud is compressed inside the satellite orbits as seen in Fig. 5b, giving somewhat

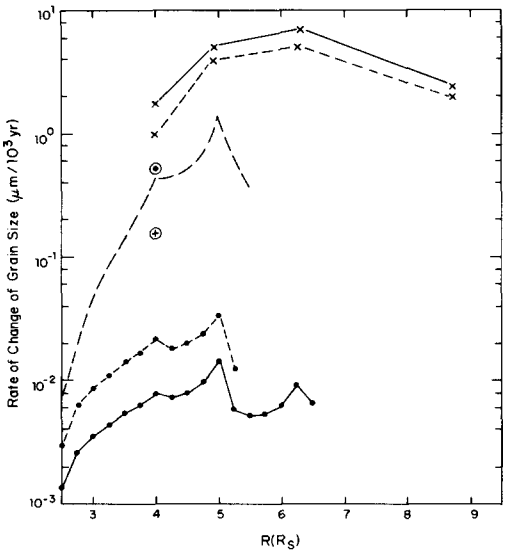

FIG. 7. Accretion rates and erosion rates of small objects in the neutral torus given in the satellite orbital plane: (×---×) erosion rates for hot plasma, (×—×) erosion rate total in Table 2; (●—●) accretion rates on a neutral object (trailing hemisphere calculation); (●--●) same but without charge exchange loss; (---) accretion rate on a small particle moving at the plasma corotation speed, trailing hemisphere ejection. ⊕ Pioneer erosion rate at Enceladus (Table 2). ⊙ Accretion rate of heavy ions at Enceladus.

higher densities. The neutral cloud in Fig. 5b is seen to terminate fairly sharply beyond the orbit of Rhea and the densities in the vicinity of Enceladus are seen to be about a factor of 2 larger for the trailing hemisphere ejection. Removing charge exchange again gives a similar structure with higher densities (~70 moles/cm^3 near Enceladus, ~150 moles/cm^3 near Tethys, ~80 moles/cm^3 near Dione).

From Figs. 6a and b the heavy ion source for the inner plasma torus described here is physically distinct from that for the Titan plumes (Eviatar *et al.* 1982, 1983; Eviatar 1984; Richardson *et al.* 1986). The cases displayed in Figs. 5a and b can be considered as two limits for the morphology of the neutral cloud. Based on the discussion in the text these densities are *lower limits*.

PLASMA TORUS STRUCTURE

In Fig. 8 is shown a plot of the plasma source rate in the equatorial plane vs distance from Saturn. This source is seen to have a striking structure, being highly peaked about the satellite sources. Inside about $10R_S$ the trailing hemisphere and isotropic ejection give nearly identical structures to first order. Also shown are the total ion densities for the Pioneer data and the model of Richardson and Siscoe (1988). The Pioneer data are of interest because the spacecraft spent most of its time close to the orbital plane. [The rough mass analysis on Pioneer indicated that the ion composition was changing in the region, which was not found to be the case for Voyager (Lazarus and McNutt 1983; Richardson 1986).] The Pioneer plasma densities (100 eV – 8 keV O^+) are strikingly similar to the calcu-

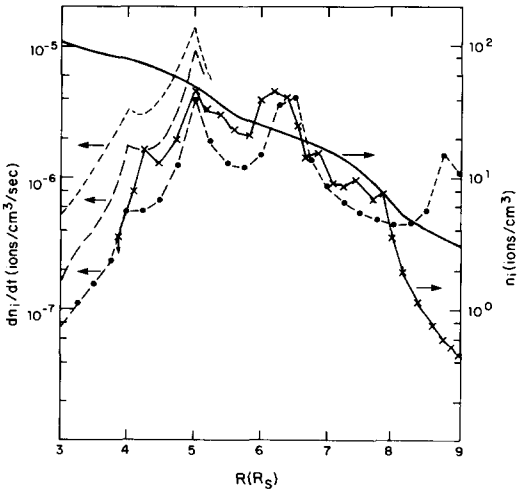

FIG. 8. Plasma source rate, dn_i/dt, calculated (left-hand axis) and heavy ion number densities, n_i (right-hand axis), in the orbital plane of the satellite, vs distance from Saturn. (Solid dark line). Richardson and Sittler (1988) model for O^+ densities, n_i, based on Voyager data averages of inbound and outbound (text). (×—×) Pioneer II heavy ion densities, n_i. Calculated heavy ion source rates (Dot-dashed line) for isotropic ejection, dn_i/dt; (long-dashed line) for isotropic ejection *without* charge exchange loss of neutrals; and (short-dashed line) for trailing hemisphere ejection *without* charge exchange.

lated source distribution, with the exception of the vicinity of Rhea, where Pioneer is farthest from the orbit plane. Strongly peaked densities near the satellite orbits are opposite to what is seen for very energetic ions (Simpson *et al.* 1980) and are also different from the observations of the Jovian plasma at the icy Galilean satellites. The structure in the heavy ion densities at the inner icy satellites of Saturn are strongly suggestive that the icy satellites are the dominant source of heavy plasma at Saturn *and* that this plasma is not fully equilibrated.

In contrast to the Pioneer data, the extrapolation of the Voyager data displays practically no structure. Various assumptions in the extrapolation procedure can lead to smoothing. For example a latitudinal gradient in $T_\perp/T_\parallel$, as discussed in Richardson (1986), might result in a reduced structure in the extrapolated densities near the equatorial plane. Beyond about $L = 4.8R_S$ the extrapolated Voyager densities exhibit some general dependence on R shown by the calculated source distribution in Fig. 8. Inside $L = 4.8R_S$ the extrapolated Voyager plasma density rises with decreasing L with $n_e \sim 100$ cm^{-3} at $L = 2.8R_S$. (The drop in the Pioneer plasma data in this region is due to the low-energy cutoff of 100 eV for the instrument.) As the vertically integrated ion source term will be proportional to the total flux content (Sittler *et al.* 1983), the decrease in the calculated source term at small R_S is of interest.

A problem with extrapolation of the plasma densities using scale height distributions is seen in Fig. 9. The z (perpendicular to orbital plane) dependence for one of the calculated source distributions is displayed at $4.5R_S$ and compared to the Voyager 2 z dependence extracted by Lazarus and McNutt (1983) near the satellite orbital plane crossing. It is seen that the standard $\exp(-z^2/H^2)$ dependence describes neither the source distribution nor the measured distribution. Lazarus and McNutt (1983) interpreted this as implying different $T_\parallel$ values vs perpendicular distance. Although the source distribution is somewhat model dependent, it is clear from Fig. 9 that the measured density dependence with z exhibits aspects of the calculated *source distribution*. Hence, the observed "scale height" may represent the sputter particle energy distribution as well as the plasma temperature.

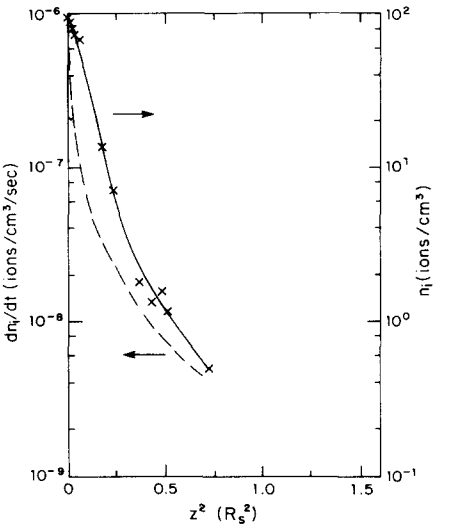

FIG. 9. z dependence (measured perpendicular to orbital plane) at $\sim 3R_S$ of the ion density, n_i (right-hand axis), and calculated ion source rate, dn_i/dt (left-hand axis): data (×) and extrapolation of Voyager 2 data (solid line) (Lazarus and McNutt 1983); (dashed line) trailing hemisphere ejection calculation of source rate ignoring charge exchange loss rate in calculating neutral number densities. Shape of curve depends on ionization rates but general trend is as shown.

The above observations imply that the heavy ion plasma is composed of "freshly produced" ions which have not experienced significant diffusion and have not become fully equilibrated. That this is likely to be the case has also been inferred by other means (Richardson *et al.* 1986). In addition, taking the ratio of the plasma production in Fig. 8 to the plasma densities in that figure, ion lifetimes $\sim 10^6$–10^7 sec are inferred. An exchange of old ions for new ions occurs at a rate directly proportional to the neutral density in Fig. 5. Using an average charge exchange cross section $\sim 10^{15}$

cm^2, as discussed earlier, the lifetime of such ions in the Enceladus–Dione torus is of the order of a year $\sim 10^6$–10^7 sec. There may be an equivalent amount of neutral H from the Saturn corona (Shemansky, private communication) also providing charge exchange targets. Therefore, charge exchange times are roughly comparable to the lifetimes inferred from Fig. 8. By contrast, the estimated diffusion times are $\sim 10^7$–10^8 sec in this region (Hood, 1983; Richardson *et al.* 1986; Paonessa and Cheng 1986) and electron–molecule recombination times at small R are $\sim 10^7$ sec (Richardson *et al.* 1986). In the vicinity of Rhea shorter lifetimes are suggested by Fig. 8, due probably to higher diffusion rates (Richardson *et al.* 1986) or possibly to intrusion of neutrals from Titan (Eviatar 1984).

Comparing the ion densities from Voyager and ion source rates in Figs. 8 and 9 at small radii ($<4.5R_S$), it is seen that much larger ion lifetimes or larger source rates (neutral densities) are required. Based on our earlier discussion, the charge exchange process in this region is less effective at removing neutrals. Setting the loss due to charge exchange to zero increases the ion source rates significantly. However, they still do not reflect the ion density distribution. As inward diffusion is not likely to be large or to produce the appropriate plasma profile we infer that there are *additional sources* of neutrals in this region. In addition to Mimas there are a number of small objects, satellites, and diffuse rings (Connerney 1987) in this region, giving, in principle, a significant surface area. However, the ion sputter yields are very small (i.e., less than one per incident O^+, Table II) so that micrometeorite bombardment of these objects dominates (Cheng *et al.* 1986). As the main ring system also gives evidence of micrometeorite bombardment (Northrop and Connerney 1987; Morfill *et al.* 1983a,b) it is possible that ring erosion can produce an inner source of heavy neutrals, hence plasma, a process to be described in a subsequent work.

The neutral densities can also reduce the density of the H^+ plasma close to the orbital plane. If ion thermal equilibrium is not established rapidly so that the H^+ pitch angles are small then any H^+ passing through the neutral torus will have a nonnegligible probability of nearly symmetric charge transfer with the heavy neutrals (H_2O, OH, O, etc.) as well as with the neutral H produced (not shown here). By contrast, new H^+ from the sputter source is distributed, on the average, at much larger distances above and below the orbit plane due to energetic dissociation of H_2O and OH and from H ejected from Saturn's atmosphere. Therefore, the ratio of sources of H^+ to charge exchange loss of H^+ near the orbital plane is relatively small.

ACCRETION RATES: E RING

It is intriguing whether or not the E-ring is a "precipitate" from the neutral water product torus inside of the orbit of Enceladus (Haff *et al.* 1983; Johnson *et al.* 1984; Cheng *et al.* 1986). In Fig. 7 are given accretion rates of H_2O on a small rotating particle orbiting about Saturn and for a similar charge particle rotating with the magnetosphere. Eliminating Enceladus as a sputter source of neutrals (Haff *et al.* 1983) changes the calculated accumulation rates in Fig. 7 by at most a factor of 2 at $4R_S$, as Tethys is an important source of neutrals in the vicinity of Enceladus. The calculated accretion rates given are considered to be the two limits for the sweeping up of the neutrals by small particles in the Saturn neutral water vapor torus. That is, very small E-ring particles are likely to be charged, which affects the dispersion of the ring particles in the Saturnian magnetosphere (Hill 1984; Morfill *et al.* 1983b). Therefore, these particles can have effective "orbital" speeds somewhere between the gravitational limit and the magnetosphere corotation limit.

Also shown are the erosion rates from Table II due to the hot plasma ions which have velocities much larger than the corota-

tion velocity. The erosion rate calculated using Pioneer data at Enceladus (Table II) is also shown because of the close proximity to the orbital plane of the measurements. The Pioneer data give a lower erosion rate at Enceladus than the hot plasma, as it does not include ions with energies larger than 8 keV. Because of the importance and the uncertainty in using the Voyager data near Enceladus (e.g., fraction of H^+ vs O^+, extrapolation to orbit plane, etc.), the Pioneer erosion rate can be considered a useful lower limit. Finally, if the grains are very fluffy and underdense at the molecular level, which is likely, the erosion rates could be even smaller (Hapke 1986; Johnson *et al.* 1985).

We also note that at very low energies the incident heavy ions do *not* sputter the small grains, but become implanted, *adding* to the grain growth. This was implied by calculating the effective yields in Table II using $Y - 1$ in Eq. (1), where Y is the measured (extrapolated) yield from Fig. 1a. The zeros in Table II indicate that this yield is less than one, so the grains can *grow* due to ion implantation inside of $\sim 3.5 R_S$. That is, in this region of the cold torus ions have low energies relative to the grains (and the LECP ion erosion rates are very uncertain). The excess energy of an implanted ion can be eventually dissipated by a number of means and the plasma electron density is sufficiently large and temperature low enough to stabilize the excess charge. The flux of low-energy ions sticking to the grains is also indicated in Fig. 7) for the case in which the E-ring particles have gravitationally controlled orbital speeds.

Based on the numbers described above, it appears clear that E-ring particles are eroded, particularly at $L > 4R_S$. However, using the Pioneer erosion rate, charged grains, trailing hemisphere ejection, and/or accumulation on the grains of low-energy ($\ll$100 eV) ions, this conclusion could change at smaller R. In addition, we have already concluded that for $R < 4R_S$ *additional sources of neutrals* are needed to describe the plasma source. This would clearly enhance the prospects for growth at small R. In this regard, Sittler *et al.* (1983) reported evidence for the depletion of superthermal electrons with energies less than 6 keV which may be explained by significant levels of submicron-sized particles or large molecules.

If ice cluster growth is to occur in this region, it can be initiated by molecular ions reacting with neutrals. This is a very different process from, for example, ice precipitation in an atmosphere. When very low energy ions impact neutral molecules the ions are attracted by the polarization force and orbit the neutrals (Johnson 1982), losing their initial momentum to the center of mass of the pair. Therefore, within about $2.7 R_S$, charge transfer does *not* necessarily lead to loss of the neutralized species from the system so that neutrals accumulate. Clustering of a neutral onto a molecular ion can be stabilized by the low-temperature electrons (Richardson *et al.* 1986) and/or by electron recombination and H ejection. Occasionally, large cluster ions may also be directly ejected from satellites (Ip 1986) and seed this process. As the clusters grow any excess energy from the "capture" of an ionic species can be dispersed throughout the quasi-bound complex for longer periods, enhancing the probability of stabilization. As the nascent E-ring particles orbit at velocities closer to the magnetosphere corotation speed, sputtering is unlikely and accretion is enhanced (Fig. 7). These considerations allow the possibility that very small particles can be formed at small R so that the E-ring might be a "stable" feature of the icy component of the present Saturnian system. The hot plasma erosion rates and neutral sources inside of $4R_S$ are the largest uncertainties in this very interesting problem.

CONCLUSIONS

The sputter production of a neutral torus of water ice products (H_2O, OH, O) is calculated using laboratory sputter data for kilo-electron volt ions and spacecraft measurements of the plasma ion and electron

densities and temperatures. This cloud is seen to form an enormous toroidal atmosphere about Saturn which coorbits with the inner icy satellites and the E-ring. The densities are such that detection from Earth is unlikely. As this torus is a source of heavy ions, we have shown here that the neutral torus morphology has been indirectly observed by spacecraft detection of the distribution of the structured heavy ion plasma close to the satellite orbit plane. That is, the source distribution of heavy ions calculated from the sputter-produced neutral torus exhibit density variations in both R and z resembling those of the heavy ion plasma as seen by Pioneer. In fact, the out-of-plane structure of this plasma (scale height) may be attributed in part to the sputtered particle energy distribution. This gives the possibility of an exciting direct connection of the plasma properties with recent laboratory measurements (Reimann *et al.* 1984) of sputter molecule energy distributions. It further complicates, however, the process of extrapolating the Voyager plasma measurement. That is, to obtain a plasma model the morphology of the source has to be included.

The ion source and neutral distributions are shown to be consistent with ion lifetimes of the order of 10^6–10^7 sec in the region of Dione and Tethys. These times are comparable to the charge exchange loss rate of ions in this region. It is also noteworthy that extrapolated and measured Voyager ion densities at radial distances $<4R_S$ exhibit a trend not reflected in the calculated ion source rates. This suggests an additional source of neutrals at small R which is much larger than the Tethys–Dione contributions in this region, such as ejecta from the outer regions of the main ring system due to micrometeorite bombardment. In this region the molecular processes controlling the local neutral cloud also change in character, as discussed, requiring more detailed accounting of the fate of neutrals.

We also examined the possibility that the E-ring is a "stable" feature of the Saturnian system, i.e., a precipitate of the neutral torus. It initially appeared that the high erosion rates by the LECP heavy ions would mitigate against this (Johnson *et al.* 1984) but the possibility of cluster growth at small R was described. For this reason and because of the likelihood of additional sources, a detailed description of the inner region of the neutral torus is both an important and an interesting problem in molecular physics, one that will be elucidated considerably by a Cassini mission.

ACKNOWLEDGMENTS

The authors thank John Richardson for helpful comments and the use of the plasma data in advance of publication. This work was supported by NASA Planetary Atmospheres Division under Grant NAGW 461 and by NASA Geology and Geophysics Division under Grant NAGW-186.

REFERENCES

BAGNENAL, F., AND J. D. SULLIVAN 1981. Direct plasma measurements in the Io torus and inner magnetosphere of Jupiter. *J. Geophys. Res.* **86,** 8447.

BAR-NUN, A. G., M. L. HERMAN, M. L. RAPPAPORT, AND YU MEKLER 1985. Sputtering of water ice at 30–140K by 0.5–6.0 keV H^+ and Ne^+ ions. *Surf. Sci.* **150,** 193–201.

BARTON, L. 1983. *Ion Erosion of the Icy Satellites of Saturn.* Master's thesis in Engineering Physics, University of Virginia, Charlottesville.

BAUM, W. A., T. KREIDL, J. A. WESTPHAL, G. E. DANIELSON, P. K. SEIDELMANN, D. PASCU, AND D. G. CURRIE 1981. Saturn's E-ring. *Icarus* **47,** 84–96.

BØTTIGER, J., J. A. DAVIES, J. L'ECUYER, N. MATSUNAMI, AND R. OLLERHEAD 1980. Erosion of frozen-gas films by MeV ions. *Radiat. Eff.* **49,** 119–124.

BRENNER, AND B. GARRISON 1986. Classical dynamics study of the ion bombardment of ice. *Phys. Rev. B* **34,** 5782–5787.

BRIDGE, H. S., *et al.* 1981. Plasma observations near Saturn: Initial results from Voyager 1. *Science* **212,** 217–224.

BRIDGE, H. S., *et al.* 1982. Plasma observations near Saturn: Initial results from Voyager 2. *Science* **215,** 563–570

BROWN, W. L., W. M. AUGUSTYNIAK, K. J. MARCANTONIO, E. H. SIMMONS, J. W. BORING, R. E. JOHNSON, AND C. T. REIMANN 1984. Electronic sputtering of low temperature molecular solids. *Nucl. Instrum. Methods B* **1,** 307–314.

CHENG, A. F., P. K. HAFF, R. E. JOHNSON, AND L. J. LANZEROTTI 1986. Interactions of Planetary Magnetospheres with the icy satellite surfaces. In *Satellites* (J. A. Burns and M. S. Matthews, Eds.), pp. 403–436. Univ. of Arizona Press, Tucson.

CHENG, A. F., AND L. J. LANZEROTTI 1978. Ice sputtering by radiation belt protons and the rings of Saturn and Uranus. *J. Geophys. Res.* **83,** 2597–2607.

CHRISEY, D. B., J. W. BORING, J. A. PHIPPS, R. E. JOHNSON, AND W. L. BROWN 1986. Sputtering of molecular gas solids by keV ions. *Nucl. Instrum. Methods B* **13,** 360–364.

CLARK, R. N., R. H. BROWN, P. D. OWENSBY, AND A. STEELE 1984. Saturn's satellites: Near infrared spectrophotometry (0.65–2.5 μm) of the leading and trailing sides and compositional implications. *Icarus* **58,** 265–281.

CLARK, R. N., F. P. FANALE, AND M. J. GAFFEY 1986. Surface composition of the natural satellites. In *Satellites* (J. A. Burns and M. S. Matthews, Eds.), pp 437–491. Univ. of Arizona Press, Tucson.

COOPER, B. H., AND T. A. TOMBRELLO 1984. Enhanced erosion of H_2O films by high energy ^{19}F ions. *Radiat. Eff.* **80,** 203–231.

CONNERNEY, J. E. P. 1987. The magnetospheres of Jupiter, Saturn and Uranus. *Rev. Geophys.* **25,** 615–638.

EVIATAR, A. 1984. Plasma in Saturn's magnetosphere. *J. Geophys. Res.* **89,** 3821–3828.

EVIATAR, A., R. L. MCNUTT, G. L. SISCOE, AND J. D. SULLIVAN 1983. Heavy ions in the outer Kronian magnetosphere. *J. Geophys. Res.* **88,** 823–831.

EVIATAR, A., G. L. SISCOE, J. D. SCUDER, E. C. SITTLER, JR., AND J. D. SULLIVAN 1982. The plumes of Titan. *J. Geophys. Res.* **87,** 8091–8096.

FRANK, L. A., B. G. BUREK, K. L. ACKERSON, J. H. WOLFE, AND J. D. MIHALOV 1980. Plama in Saturn's magnetosphere. *J. Geophys. Res.* **85,** 5695–5708.

HAFF, P. K., AND A. EVIATAR 1986. Micrometeroid impact on planetary satellites as a magnetospheric mass source. *Icarus* **66,** 258–269.

HAFF, P. K., A. EVIATAR, AND G. L. SISCOE 1983. The enigma of Enceladus. *Icarus* **56,** 426–438.

HAPKE, B. 1986. On the sputter alteration of regoliths of outer Solar System bodies. *Icarus* **66,** 270–279.

HARING, R. A., A. HARING, F. S. KLEIN, A. C. KUMMEL, AND A. E. DE VRIES 1983. Reactive sputtering of simple condensed gases by keV heavy ions. *Nucl. Inst. Methods* **211,** 529–533.

HARING, R. A., R. PEDRYS, D. J. OOSTRA, A. HARING, AND A. E. DE VRIES 1984. Reactive sputtering of simple condensed gases by keV ions II: mass spectra. *Nucl. Instrum. Methods B* **5,** 476–482.

HILL, T. W. 1984. Saturn's E-ring. *Adv. Space. Res.* **4,** 149–157.

HOOD, L. L. 1983. Radial diffusion in Saturn's radiation belts: A model analysis assuming satellite and E-ring absorption. *J. Geophys. Res.* **88,** 808–818.

HUANG, T. S., AND G. L. SISCOE 1987. Types of planetary tori. *Icarus* **70,** 366–370.

IP, W.-H 1986. Cassini instruments related to interaction between magnetosphere and surfaces. In *The Solid Bodies in the Outer Solar System.* ESA Pub. SP-242, pp. 179–194.

JOHNSON, R. E. 1982. *Introduction to Atomic and Molecular Collisions,* pp. 55, 206, 210. Plenum, New York.

JOHNSON, R. E., L. A. BARTON, J. W. BORING, W. A. JESSER, W. L. BROWN, AND L. J. LANZEROTTI 1985. Charge particle modification of ices in the Saturnian and Jovian systems. In *Ices in the Solar System* (J. Klinger *et al.*, Eds.), pp. 301–315. Reidel, Dordrecht.

JOHNSON, R. E., L. J. LANZEROTTI, AND W. L. BROWN 1984. Sputtering processes: Erosion and chemical change. *Adv. Space Res.* **4,** 41–51.

JOHNSON, R. E., AND D. STROBEL 1982. Charge exchange collisions of interest in the Io torus. *J. Geophys. Res.* **10,** 385–393.

KRIMIGIS, S. M., J. F. CARBARY, E. P. KEATH, T. P. ARMSTRONG, L. J. LANZEROTTI, AND G. GLOCKER 1983. General characteristics of hot plasma and energetic particles in the Saturnian magnetosphere: Results from the Voyager spacecraft. *J. Geophys. Res.* **88,** 8871–8892.

KRIMIGIS, S. M., *et al.* 1981. Low energy charged particles in Saturn's magnetosphere: Results from Voyager 1. *Science* **212,** 225–231.

LANZEROTTI, L. J., W. L. BROWN, K. J. MARCANTONIO, AND R. E. JOHNSON (1984). Production of ammonia-depleted surface layers on the Saturnian satellites by ion sputtering. *Nature* **312,** 139–140.

LANZEROTTI, L. J., C. G. MACLENNON, W. L. BROWN, R. E. JOHNSON, L. A. BARTON, C. T. REIMANN, J. W. GARRETT, AND J. W. BORING 1983. Implications of Voyager data for energetic ion erosion of the icy satellites of Saturn. *J. Geophys. Res.* **88,** 8765–8770; 1984a. Erratum. *J. Geophys. Res.* **89,** 9157.

LAZARUS, A. J., AND R. L. MCNUTT 1983. Low energy plasma ion observations in Saturn's magnetosphere. *J. Geophys. Res.* **88,** 8765–8770.

MILLER, J. H., W. E. WILSON, S. T. MANSON, AND M. E. RUDD 1987. Differential cross sections for ionization of water vapor by high-velocity bare ions and electrons. *J. Chem. Phys.* **86,** 157–162.

MOORE, J. M. 1984. The tectonic and volcanic history of Dione. *Icarus* **59,** 205–209.

MORFILL, G. E., E. GRUN, C. K. GOERTZ, AND T. V. JOHNSON 1983a. On the evolution of Saturn's "spokes": Theory. *Icarus* **53,** 230–235.

MORFILL, G. E., E. GRUN, AND T. V. JOHNSON 1983b. Saturn's E, G, and F rings; Modulated by the plasma sheet. *J. Geophys. Res.* **88,** 5573–5579.

NORTHROP, T. G., AND J. E. P. CONNERNEY 1987. A micrometeorite erosion model and the age of Saturn's rings. *Icarus* **70,** 124–137.

ORIENT, O. J., AND S. K. SRIVASTAVA 1984. Dissociative ionization of water by electrons. In *Proceedings, Ninth International Conference on Atomic Physics, Seattle, WA.*

PAONESSA, M., AND A. F. CHENG 1986. Limits on ion radial diffusion coefficients in Saturn's inner magnetosphere. *J. Geophys. Res.* **91,** 1391–1396.

POSPIESZALSKA, M. K., AND R. E. JOHNSON 1987. Magnetospheric ion bombardment profiles of satellites: Europa and Dione examples. Submitted for publication.

REIMANN, C. T., J. W. BORING, R. E. JOHNSON, J. W. GARRETT, K. R. FARMER, W. L. BROWN, K. J. MARCANTONIO, AND W. M. AUGUSTYNICK 1984. Ion-induced molecular ejection from D_2O ice. *Surf. Sci.* **147,** 227–240.

RICHARDSON, J. D. 1986. Thermal ions at Saturn: Plasma parameters and implications. *J. Geophys. Res.* **91,** 1381–1389.

RICHARDSON, J. D. AND A. EVIATAR 1988. Observational and theoretical evidence for anisotropies in Saturn's magnetosphere. *J. Geophys. Res.*, in press.

RICHARDSON, J. D., A. EVIATAR, AND G. L. SISCOE 1986. Satellite tori at Saturn. *J. Geophys. Res.* **91,** 8749–8755.

RICHARDSON, J. D., AND E. C. SITTLER, JR. 1988. Low energy plasma at Saturn. Submitted for publication.

SCHUTTEN, J., F. J. DETTER, H. R. MOUSTAFA, A. H. H. BOERBOOM, AND J. KISTEMAKER 1966. Electron impact ionization of H_2O. *J. Chem. Phys.* **44,** 3924–3928.

SIEVEKA, E. M., AND JOHNSON, R. E. 1982. "Thermal- and plasma-induced molecular redistribution on the icy satellites. *Icarus* **51,** 528–548.

SIEVEKA, E. M., AND R. E. JOHNSON 1984. Ejection of atoms and molecules from Io by plasma–ion impact. *Astrophys. J.* **287,** 418–426.

SIMPSON, J. A., T. S. BASTIAN, D. L. CHENETTE, R. B. MCKIBBAN, AND K. R. PYLE 1980. The trapped radiations of Saturn and their absorption by Satellites and rings. *J. Geophys. Res.* **85,** 5731–5762.

SITTLER, E. C., JR., K. W. OGILVIE, AND J. D. SCUDDER 1983. Survey of low energy plasma electrons in Saturn's magnetosphere: Voyager 1 and 2. *J. Geophys. Res.* **88,** 8847–8870.

SITTLER, E. C., JR., AND D. STROBEL 1987. Io plasma torus electrons: Voyager 1. *J. Geophys. Res.* **92,** 5741–5762.

SMYTH, W. H. 1979. Na neutral cloud. *Astrophys. J.* **234,** 1148–1160.

SMYTH, W. H., AND D. E. SHEMANSKY 1983. Escape and ionization of atomic oxygen from Io. *Astrophys. J.* **271,** 865–875.

STEVENSON, D. J. 1982. Volcanism and igneous processes in small icy satellites. *Nature* **298,** 142–144.

WU, F. M., D. L. JUDGE, AND R. W. CARSON 1980. Observations of Extreme Ultraviolet Emissions from the Saturnian Plasmasphere. *J. Geophys. Res.* **11,** 5853–5856.